Photoelectron emission from metal surfaces by ultrashort laser pulses

M. N. Faraggi,[1] M. S. Gravielle,[1,2] and V. M. Silkin[3]
[1]*Instituto de Astronomía y Física del Espacio, CONICET, Casilla de Correo 67, Sucursal 28, 1428 Buenos Aires, Argentina*
[2]*Departamento de Física, FCEN, Universidad de Buenos Aires, Buenos Aires, Argentina*
[3]*Donostia International Physics Center DIPC, P. Manuel de Lardizabal 4, 20018 San Sebastián, Spain*
(Received 15 November 2005; published 3 March 2006)

Electron emission from metal surfaces produced by short laser pulses is studied within the framework of the distorted-wave formulation. The proposed approach, named surface-Volkov (SV) approximation, makes use of the band-structure based (BSB) model and the Volkov phase to describe the interaction of the emitted electron with the surface and the external electric field, respectively. The BSB model provides a realistic representation of the surface, based on a model potential that includes the main features of the surface band structure. The SV method is applied to evaluate the photoelectron emission from the valence band of Al(111). Angular and energy distributions are investigated for different parameters of the laser pulse, keeping in all cases the carrier frequency larger than the plasmon one.

DOI: 10.1103/PhysRevA.73.032901 PACS number(s): 79.20.Ds, 61.80.Ba, 79.60.−i

I. INTRODUCTION

The interest in the study of laser-surface interactions is motivated by the latest developments in laser applications, which include irradiation over metal, plastic, and biological solids [1]. In particular, the photoelectron emission induced by laser pulses from solid surfaces has become a promising tool to determine the carrier-envelope phase of the pulse [2,3].

The present work focuses on the electron emission produced by the interaction of an intense few-cycle laser pulse with a metal surface. This process was recently studied within the density functional theory in Ref. [2] by solving the time-dependent Khon-Sham equations numerically. The method, albeit precise, involves a hard computational task. For this reason we propose an approach based on the use of Volkov-type wave functions [4], which requires less computational efforts. We introduce a time-dependent distorted-wave method, here named surface-Volkov (SV) approximation, which combines the band-structure based (BSB) [5] model with the phase of the Volkov wave function to represent the final distorted electronic state. The BSB theory is based on the model potential proposed by Chulkov *et al.* [6], which incorporates information about the band structure of the solid, providing an accurate description of the one-electron states at a metal surface. This potential has been successfully applied in several branches [7–10]. The Volkov wave function is the exact solution of the Schrödinger equation for a free electron in an electromagnetic field [11], and it has been extensively used to compute atomic processes driven by monochromatic laser fields [12]. Therefore, the SV approach is expected to include the main aspects of the interaction of the ejected electron with both, the surface and the applied electric field.

The proposed method is employed to evaluate the electron emission from the valence band of Al(111) due to the interaction with an ultrashort and intense laser pulse. The study is confined to large frequencies of the laser field, for which the influence of the surface induced potential on the emitted electron can be neglected. Angular and energy distributions of ejected electrons are analyzed for different durations of the pulse, allowing from zero to several oscillations of the field. The paper is organized as follows. In Sec. II we describe the theoretical model, in Sec. III results are presented and discussed, and in Sec. IV conclusions are summarized.

Atomic units are used throughout unless otherwise stated.

II. THEORY

We consider a short laser pulse, characterized by the electric field $\mathbf{F}(t)$, which impinges grazingly on a metal surface (S). As a result of the interaction with the external electric field, an electron (e) of the conduction band of the solid, initially in the state i, is excited to a final state f. The frame of reference is placed at the position of the crystal border, which is shifted a half interplanar distance with respect to the topmost atomic layer. The $\hat{z}$ axis is fixed perpendicular to the surface, aiming towards the vacuum region.

The temporal evolution of electronic state $\Psi(\mathbf{r},t)$, in the presence of the external field $\mathbf{F}(t)$, is determined by the time-dependent Schrödinger equation

$$i\frac{\partial\Psi(\mathbf{r},t)}{\partial t}=[H_0+V_L(\mathbf{r},t)+V_{ind}(\mathbf{r},t)]\Psi(\mathbf{r},t), \qquad (1)$$

where $\mathbf{r}$ is the position vector of the active electron e and $H_0=-\nabla_{\mathbf{r}}^2/2+V_S$ is the unperturbed Hamiltonian, with V_S the surface-electron interaction. The potential $V_L(\mathbf{r},t)=\mathbf{r}\cdot\mathbf{F}(t)$ represents the interaction with the laser field, expressed in the length gauge, and $V_{ind}(\mathbf{r},t)$ denotes the induced surface potential, created by the time-dependent density fluctuations produced by the external field.

To represent the surface interaction V_S we employ the BSB model [6], which describes appropriately the main characteristics of the surface band structure, modeling the surface as a finite and smooth barrier. Within the BSB model, translational invariance in the plane parallel to the surface is assumed, and the eigenfunctions of H_0 are expressed as

$$\Phi_{\mathbf{k}_s,n}(\mathbf{r},t) = \frac{1}{2\pi}\exp(i\mathbf{r}_s\cdot\mathbf{k}_s)\phi_n(z)\exp(-iE_{k_s,n}t), \quad (2)$$

where $\mathbf{r}\equiv(\mathbf{r}_s,z)$ has been decomposed in its components parallel and perpendicular to the surface, $\mathbf{k}_s$ denotes the parallel electron momentum, and $E_{k_s,n}=k_s^2/2+\varepsilon_n$ is the eigenenergy, with $k_s=|\mathbf{k}_s|$. The one-dimensional functions $\phi_n(z)$ and their corresponding eigenenergies ε_n are obtained solving the one-electron Schrödinger equation associated with the one-dimensional model potential of Ref. [5] in a slab geometry [13]. The function $\phi_n(z)$ has the following representation:

$$\phi_n(z) = \frac{1}{\sqrt{L}}\sum_{j=-N}^{N} a_n(j)\exp\left(i\frac{2\pi j}{L}\tilde{z}\right), \quad (3)$$

where L is a normalization length and $2N+1$ is the number of basis functions. The coordinate $\tilde{z}=z+d_S$ is measured with respect to the center of the slab, which is placed at a distance d_S from the surface edge, and the coefficients $a_n(j)$ are numerically evaluated.

As a consequence of the momentum conservation, the description of photoelectron emission by an electric field parallel to the surface requires the inclusion of the parallel recoil of the crystal lattice. Then, the parallel invariance of the BSB surface interaction restricts the application of the SV approximation to electric fields normal to the surface plane. In this work we consider a laser pulse represented by a time-dependent electric field linearly polarized along the $\hat{z}$ axis. This is compatible with the approximately grazing incidence of the light on the surface. The temporal profile of the pulse is defined as

$$F(t) = F_0\sin(\omega t+\varphi)\sin^2(\pi t/\tau) \quad (4)$$

for $0<t<\tau$, and 0 elsewhere, with τ the pulse duration, ω the carrier frequency, φ the carrier-envelope phase, and F_0 the maximum field strength.

A. SV transition amplitude

From the BSB electronic state, we derive the SV distorted-wave function by introducing the phase corresponding to the well-known Volkov state [11]. For the final channel, it reads

$$\chi_f^{(SV)-}(\mathbf{r},t) = \Phi_{\mathbf{k}_{fs},n_f}(\mathbf{r},t)\exp[iD^-(z,t)], \quad (5)$$

where $\Phi_{\mathbf{k}_{fs},n_f}$ is the final unperturbed state defined by Eq. (2), and

$$D^-(z,t) = \frac{z}{c}A^-(t) - \beta^-(t) \quad (6)$$

is the Volkov phase introduced by the electromagnetic field, with the light velocity c. In Eq. (6), $A^-(t)$ represents the vector potential, which is related to the electric field as

$$A^-(t) = -c\int_{+\infty}^{t} dt' F(t'), \quad (7)$$

and $\beta^-(t)=(2c^2)^{-1}\int_{+\infty}^{t}dt'[A^-(t')]^2$ is associated with the ponderomotive energy. Note that in the definition of $A^-(t)$ we have set $A^-(+\infty)=0$ to represent properly the final (incoming) asymptotic conditions, i.e., $\chi_f^{(SV)-}(\mathbf{r},t)\to\Phi_{\mathbf{k}_{fs},n_f}(\mathbf{r},t)$ for $t\to+\infty$. Under the impulsive hypothesis [14–16], the wave function $\chi_f^{(SV)-}$ can be considered as an approximate solution of the time-dependent Schrödinger equation given by Eq. (1). It should be particularly valid for large frequencies, for which the quiver amplitude $\alpha_0=F_0/\omega^2$ is small in comparison with the system dimensions.

By employing $\chi_f^{(SV)-}$ within the usual time-dependent distorted-wave formalism [17], the post form of the SV transition amplitude reads

$$T_{fi}^{(SV)} = a_{fi} - i\int_{-\infty}^{+\infty} dt\langle\chi_f^{(\mathrm{SV})-}(t)|W_f^{\dagger}(t)|\Phi_{\mathbf{k}_{is},n_i}(t)\rangle, \quad (8)$$

where

$$a_{fi} = \lim_{t\to-\infty}\langle\chi_f^{(SV)-}(t)|\Phi_{\mathbf{k}_{is},n_i}(t)\rangle \quad (9)$$

is the *sudden* transition amplitude and $\Phi_{\mathbf{k}_{is},n_i}$ is the initial unperturbed state given by Eq. (2). The potential $W_f(t)$ is the distortion potential corresponding to the final channel, which satisfies $[H(t)-id/dt]|\chi_f^{(SV)-}(t)\rangle=W_f(t)|\chi_f^{(SV)-}(t)\rangle$. In Eq. (8), the term a_{fi} represents a simple step process and has been found null for electronic transitions from the surface. Consequently, within the SV approximation, the photoionization process is described through the time integral over all intermediate transitions involved in the second term of Eq. (8).

In the present article we limit the ω values to the range $\omega>\omega_s$, where ω_s is the surface plasmon frequency. For such high frequencies, the induced surface potential outside the solid is small compared with V_L, and its effect on the ejected electron can be neglected. Then, by dropping the contribution of V_{ind} from the distortion potential W_f, the SV transition amplitude approximates

$$T_{fi}^{(SV)} = -i\int_{-\infty}^{+\infty} dt\langle\chi_f^{(SV)-}(\mathbf{r},t)|V_L(t)|\Phi_{\mathbf{k}_{is},n_i}(\mathbf{r},t)\rangle. \quad (10)$$

After some algebra, it becomes an analytical closed-form given by

$$T_{fi}^{(SV)} = \delta(\mathbf{k}_{fs}-\mathbf{k}_{is})R(n_f,n_i), \quad (11)$$

where the δ function expresses the parallel momentum conservation and

$$R(n_f,n_i) = i\frac{\pi}{L}\sum_{j,j'=-N}^{N} a_{n_f}^*(j)a_{n_i}(j')\exp(-iQ_{jj'}d_S)G_{jj'}, \quad (12)$$

with $Q_{jj'}=(2\pi/L)(j-j')$. The factor $G_{jj'}$ is defined as

$$G_{jj'} = \sum_{t_e}\frac{2\Delta\varepsilon+Q_{jj'}^2}{|F(t_e)|}\exp[i\Delta\varepsilon t_e + i\beta^-(t_e)], \quad (13)$$

where $\Delta\varepsilon=\varepsilon_{n_f}-\varepsilon_{n_i}$ is the transferred perpendicular energy, and the times t_e are the emission times for which the equation

$$Q_{jj'} + \frac{1}{c}A^{-}(t_e) = 0, \tag{14}$$

associated with the z-momentum transfer, is satisfied.

B. SV emission probability

The differential emission probability can be straightforwardly derived from Eq. (11) as

$$\frac{dP^{(SV)}}{dE_f d\Omega_f} = \rho_e k_f \sum_i |T_{fi}^{(SV)}|^2, \tag{15}$$

where $E_f \equiv E_{k_{fs},n_f}$ and Ω_f are the energy and direction corresponding to the final electron momentum $\mathbf{k}_f$, the sum indicates the addition over of all possible initial states i, and $\rho_e=2$ takes into account the spin states. However, as the final electronic state $\Phi_{\mathbf{k}_{fs},n_f}$ displays a well defined momentum only in the direction parallel to the surface plane, in order to obtain the differential emission probability it is necessary to define an *effective* electron momentum perpendicular to the surface as $k_{fz}=\sqrt{2\varepsilon_{n_f}}$. Employing the usual treatment for the square of the δ function [14,18], the SV differential probability reads

$$\frac{dP^{(SV)}}{dE_f d\Omega_f} = k_f \lambda_{k_{fz}} \rho_e \sum_{n_i} |R(n_f,n_i)|^2 \Theta(E_W + \varepsilon_{n_i}) \Theta(\tilde{k}_{n_i} - k_{fs}), \tag{16}$$

where $k_f=(k_{fs}^2+k_{fz}^2)^{1/2}$ is the final electron momentum and $\lambda_{k_{fz}}$ is the density of final electronic states with perpendicular momentum k_{fz}. The first unitary Heaviside function in the right hand of Eq. (16), $\Theta(E_W+\varepsilon_{n_i})$, restricts the initial states to those contained inside the Fermi sphere, with E_W the work function. While the second Heaviside function, $\Theta(\tilde{k}_{n_i}-k_{fs})$, with $\tilde{k}_{n_i}=\sqrt{-2(E_W+\varepsilon_{n_i})}$, limits the range of final parallel momenta, as a result of the momentum conservation imposed by the delta function in Eq. (11).

III. RESULTS

We apply the SV approximation to evaluate the electron emission from the valence band of Al(111) produced by the grazing incidence of ultrashort laser pulses. The following parameters are employed to describe the aluminum surface: the Fermi energy $E_F=0.414$ a.u., the work function $E_W=0.156$ a.u., the interplanar distance 4.388 a.u., and the surface plasmon frequency $\omega_s=0.4$ a.u. To solve the one-dimensional Schrödinger equation associated with the BSB model, in Eq. (3) we used a basis of plane waves with $N=170$, the width of the unit cell $L=394.92$ a.u., and the distance between the crystal border and the film center $d_S=155.77$ a.u.

Two different intensities of the field, $F_0=0.05$ and 0.1 a.u. are considered in this work. Both of them correspond to a range of strong fields but still in the perturbative regime, in which the saturation has not been reached yet [12]. Even though these high intensities could not be withstood by the material, they have been used as a limit case for the theory, allowing us to compare with similar results for ionization of atomic hydrogen [19]. Except in Fig. 4, where the effect of the phase was investigated, all calculations were made for symmetric pulses, with $\varphi=-\omega\tau/2+\pi/2$.

In the present work, carrier frequencies ω larger than the surface plasmon frequency ω_s are considered. For Al targets this condition reduces the range of application of the SV theory to photoemission processes with Keldysh parameter, $\gamma=\omega\sqrt{E_W}/F_0$ [20], larger than one (weak-field regime). We have varied the values of τ from subfemtoseconds to femtoseconds [21] so that the field performs from no to many oscillations inside the envelope.

In the BSB model, for each positive energy ε_{n_f} two functions ϕ_{n_f} can be associated: the symmetric and the antisymmetric one (classified according to symmetry properties with respect to a plane parallel to the surface and placed in the middle of the slab). Then, the wave functions given by Eq. (3) do not allow to distinguish the internal ionization process—associated with electrons emitted inside the solid—from the external ionization process, which corresponds to the emission of electrons towards the vacuum semispace. As a first estimation we consider that electrons ejected to the vacuum region are about 50% of the total ionized valence electrons [5]. This assumption will be revised only for a particular case by taking the final wave function corresponding to external emission as a lineal combination of the symmetric and antisymmetric functions [22].

A. Angular distribution

As a result of the azimuthal invariance of the problem, the angular distribution of ejected electrons given by Eq. (16) depends only on the elevation angle θ_e, which is measured with respect to the surface plane. We start the analysis of the proposed method by considering laser pulses with $F_0=0.1$ a.u. and $\omega=1$ a.u. In Fig. 1 we plot the differential emission probability, as a function of the final electron energy, for three ejection angles: $\theta_e=30$, 45, and 90°. Two different values of τ are considered: (a) $\tau=4$ a.u. and (b) $\tau=40$ a.u. The first case, $\tau=4$ a.u., corresponds to an ultrashort pulse in which the field does not perform oscillations. The mechanism behind the ionization process for nonoscillating fields is usually associated with the collisional regime because of the similarities between the electromagnetic field of the laser pulse and that produced by the grazing impact of a fast ion. Resembling ion-surface collisions [5], the emission probabilities of Fig. 1(a) decrease smoothly as the electron velocity increases, displaying only a maximum at very low electron energies.

In Fig. 1(b) we show results for a longer pulse, $\tau=40$ a.u., in which the laser field performs several (approximately five) oscillations inside the envelope. In this case the electron spectra present peaks whose number and position vary with the emission angle. These peaks are not directly related to the above-threshold-ionization (ATI) [12] maxima, which should be regularly spaced as a function of the perpendicular energy. The structures displayed in Fig. 1(b) can be associated instead with quantum interferences between photoelectrons with a same final kinetic energy but different

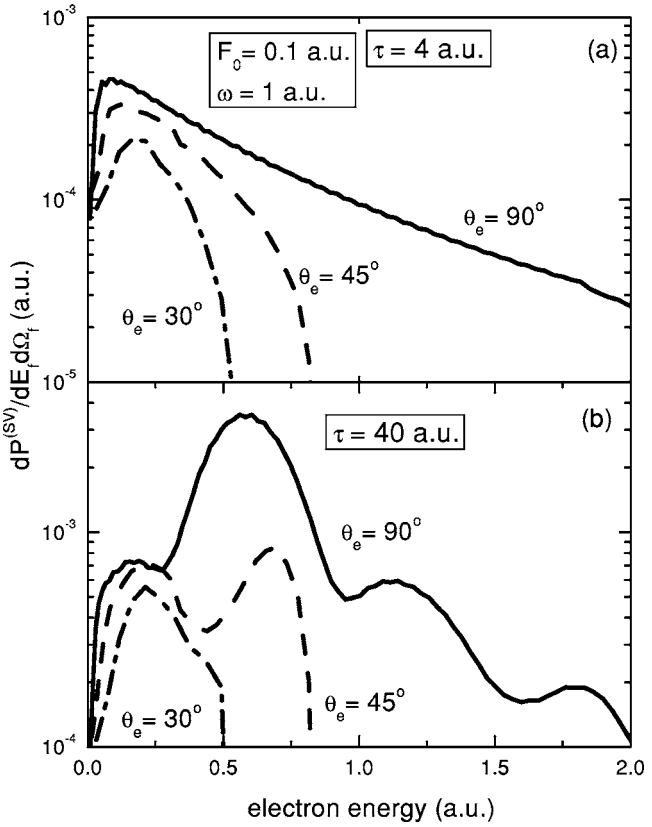

FIG. 1. Photoelectron emission probability from the valence band of Al(111), as a function of the electron energy, for three different ejection angles: θ_e=30°, 45°, and 90°. The parameters of the laser field are: F_0=0.1 a.u. and ω=1 a.u., and the duration of the pulse is: (a) τ=4 a.u. and (b) τ=40 a.u.

emission times [23,24]. Within the SV approximation, the transition from an initial to a final state occurs at the times t_e when the classical momentum transferred by the external field, $c^{-1}A^-(t_e)\hat{z}$, coincides with the perpendicular momentum gained by the electron, as expressed by Eq. (14). Then, for a given normal transferred momentum there are different times (or paths) that contribute to the electronic transition, producing interference effects.

As observed in Figs. 1(a) and 1(b), photoelectrons are mainly ejected in the direction perpendicular to the surface, which corresponds to the orientation of the external field. Besides, since the electron does not gain parallel momentum during the interaction, k_{fs} keeps within the Fermi sphere, as expressed by the last Heaviside function in Eq. (16). For this reason, the energies E_f reached by electrons ejected in a given direction θ_e are limited to be $E_f < E_F \cos^{-2}\theta_e$. Then, the range of final electron energies diminishes when the emission angle decreases, and only slow electrons with velocity lower than the Fermi one are ejected parallel to the surface.

To study the influence of the number of the cycles contained inside the envelope, we increase the duration of the pulse to let the laser field perform many oscillations in the time interval $[0,\tau]$. Electron distributions for a pulse with duration τ=100 a.u. and for different ejection angles are shown in Fig. 2, considering the same intensity and frequency of the laser field that in the previous figure. When the number of the cycles augments, the laser frequency ω tends to the photon energy, and thus, the ionization process is expected to correspond to the multiphoton regime [25]. From Fig. 2, for the angle θ_e=90° the emission probability displays two broad structures, whose perpendicular energies differ approximately in the photon energy (ω=1 a.u.). Such structures can be ascribed to the multiphoton ionization mechanism. But overlaying them, the spectrum displays an additional oscillatory pattern which could again be related to interference between different electron paths. Note that for long times τ, the electron has enough time to move inside the solid, interacting with several atomic planes before being emitted, something that might produce additional interference effects.

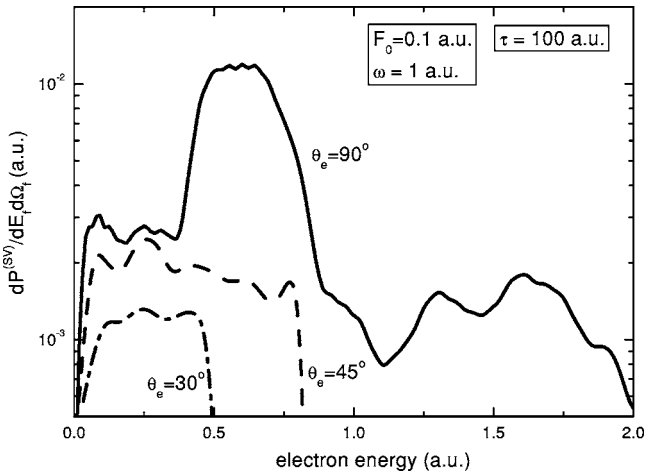

FIG. 2. Similar to Fig. 1 for a laser pulse with a duration τ=100 a.u.

With the aim of revising our estimation about the percentage of ionized electrons that are ejected towards the vacuum, we built a final wave function associated with the external ionization (EI) process as a lineal combination of the symmetric and antisymmetric ϕ_{n_f} states [22]. The coefficients of this transformation were obtained by matching the final wave function with the one corresponding to the EI process for the jellium surface potential [Eq. (A4) of Ref. [26]], considering an arbitrary position in the vacuum side, far from the surface. EI results for perpendicular emission (θ_e=90°) are plotted in Fig. 3 for a duration of the pulse τ=40 a.u., comparing them with the previous values obtained by considering that only half of the ionized electrons is ejected outside the solid. We found that for oscillating fields both procedures give similar probabilities, but some differences were observed in the collisional regime. The small pattern displayed by the EI probability in Fig. 3 might be related to the use of a discrete base to represent the final electron state.

Finally, we investigate the dependence of the photoelectron emission on the carrier-envelope phase of the pulse. While in Ref. [2] the influence of φ can be observed in the time-resolved electron emission probability, within a distorted-wave formulation, such as the SV approximation, the effect of the phase becomes evident in the electron emission spectrum. In Fig. 4 we display electron distributions for

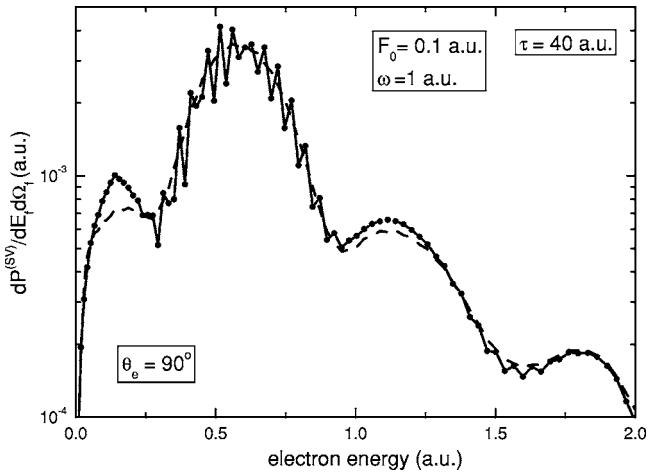

FIG. 3. Electron emission probability, as a function of the electron energy, for the ejection angle $\theta_e=90°$. The parameters of the laser field are: $F_0=0.1$ a.u., $\omega=1$ a.u., and $\tau=40$ a.u. Dashed line, similar to Fig. 1; solid line (full circles), results including EI asymptotic conditions, as explained in the text.

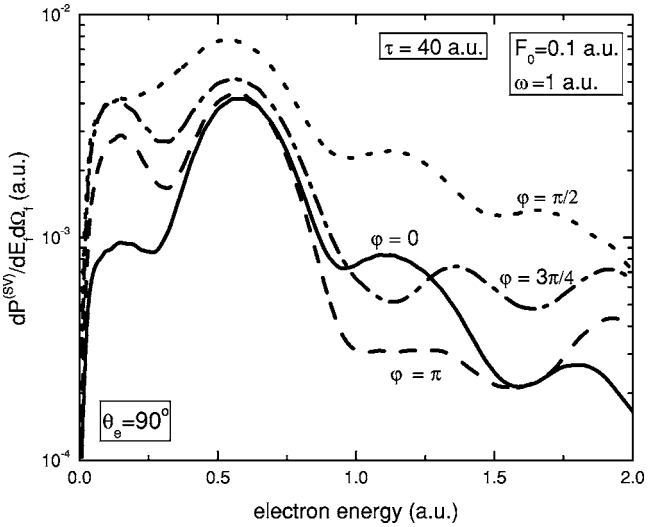

FIG. 4. Electron emission probability, as a function of the electron energy, for the ejection angle $\theta_e=90°$, considering different carrier-envelope phases. The parameters of the laser field are: $F_0=0.1$ a.u., $\omega=1$ a.u., and $\tau=40$ a.u. Solid line, $\varphi=0$; dotted line, $\varphi=\pi/2$; dashed-dotted line, $\varphi=3\pi/4$; dashed line, $\varphi=\pi$.

$\theta_e=90°$ and different phases φ, fixing the parameters of the laser—intensity, frequency, and duration—the same as in Fig. 3. We found that the electron spectrum corresponding to perpendicular ejection is strongly modified by the carrier-envelope phase. The positions and heights of the secondary maxima change noticeably for different values of φ, although the energy position of the principal maximum remains invariable. Therefore, it is expected that the measurement of electron distributions produced by ultrashort laser pulses provides useful information about the carrier-envelope phase of the pulse.

B. Energy distribution

The energy distribution of emitted electrons, $dP^{(SV)}/dE_f$, is obtained from Eq. (16) by integrating over the ejection direction Ω_f. In Fig. 5 we show emission probabilities corresponding to the field parameters $F_0=0.1$ a.u. and $\omega=1$ a.u., again for two pulse durations (a) $\tau=4$ a.u. and (b) $\tau=40$ a.u. For $\tau=4$ a.u. the laser field does not oscillate, and thus, for every transferred momentum $Q_{jj'}$ there is a unique value of t_e that satisfies Eq. (14). In this regime, the energy distribution does not displays signatures of interference; the probability decreases smoothly as a function of the electron energy, as also observed in Fig. 1(a). But when the duration of the pulse augments, allowing the pulse to perform several oscillations, interference effects arise in the spectrum [Fig. 5(b)]. Notice that even though the general features of the energy distribution of Fig. 5(b) are similar to those obtained for ionization of atomic hydrogen (Fig. 3 of Ref. [19]), in the case of surface ionization the spacing between maxima depends strongly on τ, tending to the photon energy only for long pulses.

Energy distributions corresponding to a weaker field, with the maximum strength $F_0=0.05$ a.u., are plotted in Fig. 6 for

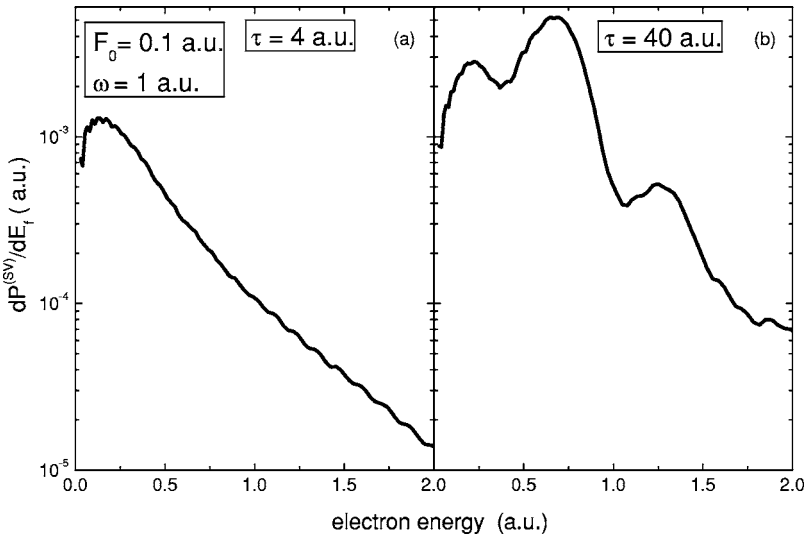

FIG. 5. Energy distribution of emitted electrons, as a function of the electron energy, for a laser field with $F_0=0.1$ a.u. and $\omega=1$ a.u. The duration of the pulse is: (a) $\tau=4$ a.u. and (b) $\tau=40$ a.u.

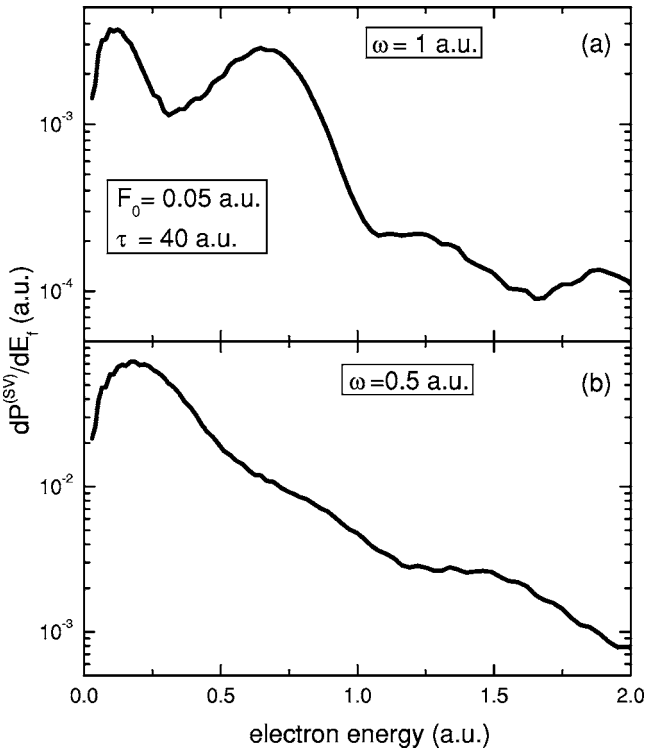

FIG. 6. Similar to Fig. 5 for a laser pulse with a maximum strength F_0=0.05 a.u., a pulse duration τ=40 a.u., and a carrier frequency (a) ω=1 a.u. and (b) ω=0.5 a.u.

a pulse duration τ=40 a.u., considering two different frequencies: (a) ω=1 a.u. and (b) ω=0.5 a.u. Comparing Figs. 6(a) and 5(b) we find that when the intensity of the field decreases, the height of the peaks diminishes, while their energy positions stay roughly invariable. But when the laser frequency is divided by two, as in Fig. 6(b), the emission probability increases and the position of the second maximum is shifted towards higher energies. The probability increase for decreasing ω values is associated with the augment of the perpendicular transferred momentum, which is determined by the vector potential A^-, as given by Eq. (14). A similar behavior is also observed in photoelectron emission from atoms for photon energies larger than the ionization potential [27,28]. In addition, in the case considered in Fig. 6(b) the laser field performs just only two oscillations. Consequently, the peaks of the energy distribution begin to disappear, tending to the collisional regime. This supports the idea that for few-cycles laser pulses, the maxima of the electronic spectrum are not related to the usual ATI peaks but are associated with interference patterns.

IV. CONCLUSIONS

We have proposed a distorted-wave method, the SV approximation, to deal with the photoelectron emission from metal surfaces induced by ultrashort laser pulses. The SV approach describes the main characteristics of the surface interaction in the initial and final channels, while the dynamics of the electron movement during the interaction time is governed by the laser field.

The SV approximation constitutes a computational inexpensive approach, whose predictions are expected to be reliable as long as the perturbative conditions hold. It allows us to evaluate angular and energy distributions of emitted electrons for laser pulses ranging from the collisional to multiphoton regimes. Even though in this work we have considered frequencies of the laser field larger than the plasmon frequency, for which the effect of the induced surface potential can be neglected, we plan to include the induced potential derived from the BSB model (with lineal response theory) in order to extend the application of the theory for lower frequencies of the laser field.

[1] Z. L. Chen, J. Zhang, T. J. Liang, H. Teng, Q. L. Dong, Y. T. Li, Z. M. Sheng, L. Z. Zhao, and X. W. Tang, J. Phys. B **37**, 539 (2004).
[2] C. Lemell, X.-M. Tong, F. Krausz, and J. Burgdörfer, Phys. Rev. Lett. **90**, 076403 (2003).
[3] A. Apolonski, P. Dombi, G. G. Paulus, M. Kakehata, R. Holzwarth, Th. Udem, Ch. Lemell, K. Torizuka, J. Burgdörfer, T. W. Hänsch, and F. Krausz, Phys. Rev. Lett. **92**, 073902 (2004).
[4] H. D. Jones and H. R. Reiss, Phys. Rev. B **16**, 2466 (1977).
[5] M. N. Faraggi, M. S. Gravielle, and V. M. Silkin, Phys. Rev. A **69**, 042901 (2004).
[6] E. V. Chulkov, V. M. Silkin, and P. M. Echenique, Surf. Sci. **391**, L1217 (1997); **437**, 330 (1999).
[7] E. V. Chulkov, I. Sarría, V. M. Silkin, J. M. Pitarke, and P. M. Echenique, Phys. Rev. Lett. **80**, 4947 (1998).
[8] J. Kliewer, R. Berndt, E. V. Chulkov, V. M. Silkin, P. M. Echenique, and S. Crampin, Science **288**, 1399 (2000).
[9] T. Hecht, H. Winter, A. G. Borisov, J. P. Gauyacq, and A. K. Kazansky, Phys. Rev. Lett. **84**, 2517 (2000).
[10] P. M. Echenique, R. Berndt, E. V. Chulkov, Th. Fauster, A. Goldmann, and U. Höfer, Surf. Sci. Rep. **52**, 219 (2004).
[11] D. M. Volkov, Z. Phys. **94**, 250 (1935).
[12] H. R. Reiss, Phys. Rev. A **22**, 1786 (1980); **65**, 055405 (2002); A. Becker and F. H. M. Faisal, J. Phys. B **38**, R1 (2005).
[13] V. M. Silkin, J. M. Pitarke, E. V. Chulkov, and P. M. Echenique, Phys. Rev. B **72**, 115435 (2005).
[14] M. R. C. McDowell and J. P. Coleman, *Introduction to the Theory of Ion-Atom Collisions*, 1st edition (North-Holland, 1970).
[15] J. E. Miraglia, J. Phys. B **15**, 4205 (1982).
[16] J. E. Miraglia and J. Macek, Phys. Rev. A **43**, 5919 (1991).
[17] D. P. Dewangan and J. Eichler, Phys. Rep. **247**, 59 (1997).
[18] C. J. Joachain, *Quantum Collisional Theory*, 1st edition (North-Holland, 1975).
[19] P. Macri, J. E. Miraglia, and M. S. Gravielle, J. Opt. Soc. Am. B **20**, 1801 (2003).

[20] L. V. Keldysh, Sov. Phys. JETP **20**, 1307 (1965).
[21] M. Nisoli, S. de Silvesti, O. Svelto, R. Szipcs, K. Ferencz, Ch. Spielmann, S. Sartania, and F. Krausz, Opt. Lett. **22**, 522 (1997).
[22] M. N. Faraggi, M. S. Gravielle, M. Alducin, J. I. Juaristi, and V. M. Silkin, Phys. Rev. A **72**, 012901 (2005).
[23] C. C. Chirila and R. M. Potvliege, Phys. Rev. A **71**, 021402(R) (2005).
[24] G. F. Gribakin and M. Yu. Kuchiev, Phys. Rev. A **55**, 3760 (1996).
[25] F. H. M. Faisal, *Theory of Multiphoton Processes* (Plenum Press, New York, 1987).
[26] M. S. Gravielle, Phys. Rev. A **58**, 4622 (1998).
[27] C. Cohen-Tannoudji, J. Dupont-Roc, and G. Grynberg, *Atom-Photon Interactions (Basic Processes and Aplications)* (Wiley Science Paperback Series, New York, 1998).
[28] G. Duchateau, E. Cormier, and R. Gayet, Phys. Rev. A **66**, 023412 (2002).